

Beam alignment for scanning beam interference lithography

Carl G. Chen,* Ralf K. Heilmann, Chulmin Joo, Paul T. Konkola, G. S. Pati, and Mark L.

Schattenburg

Massachusetts Institute of Technology, Cambridge, Massachusetts 02139

Abstract

By interfering two small diameter Gaussian laser beams, scanning beam interference lithography (SBIL) is capable of patterning linear gratings and grids in resist while controlling their spatial phase distortions to the nanometer level. Our tool has a patterning area that is up to 300 mm in diameter. The motive for developing SBIL is to provide the semiconductor industry with a set of absolute metrology standards, but the technology is easily adaptable to other important applications such as the making of high precision optical encoders. In this paper, we describe a novel system for carrying out automated beam alignment for SBIL. Our design goals require tight alignment tolerances, where beam position and angle alignment errors must be controlled to $\sim 10 \mu\text{m}$ and $\sim 10 \mu\text{rad}$, respectively. We describe our system setup, and discuss the so-called iterative beam alignment principle, focusing specifically on deriving a mathematical formalism that can guide the development of similar systems in the future. Repeatability experiments demonstrate that our system fulfills the alignment requirements for nanometer-level SBIL writing.

*Electronic mail: gangchen@mit.edu

I. INTRODUCTION

Scanning beam interference lithography (SBIL) is designed to produce close-to-ideal linear gratings over large substrates, e.g., 300 mm-diameter wafers, while controlling the nonlinear spatial phase distortions to the nanometer level. The concept and the system architecture for SBIL have been introduced elsewhere.^{1,2} To realize the design goals, we must control and correct various error sources, alignment-induced phase error being one of them. Assuming that an unflat substrate is mounted on a vacuum chuck, if angles of incidence in the two arms are unbalanced by an amount δ (Fig. 1), the direction along which interference fringes orient will deviate from the normal to the vacuum chuck by an amount $\delta/2$. Due to the intrinsic substrate thickness variation, this slight tilt would introduce a phase error to the written grating. For instance, if the substrate thickness varies by $20\ \mu\text{m}$, one can verify that an unbalance of $\delta = 10\ \mu\text{rad}$ introduces 0.1 nm of phase error, regardless of the grating period.

To obtain good interference fringe contrast, beam position overlap is also very important. A general rule of thumb is to overlap the two beam centroids to roughly 1% of the beam spot radius, i.e., for a radius of 1 mm, the centroids must be overlapped to within $\sim 10\ \mu\text{m}$ of each other.

In addition, during SBIL wavefront metrology and fringe period metrology,^{2,3} or in the so-called reading mode,⁴ the two interfering beams must align so as to be coincident upon photo-sensors after traversing metrology optics mounted on the stage.

II. SYSTEM DESCRIPTION

In order to steer a laser beam in the substrate plane in four degrees of freedom, i.e., x , y , θ and ϕ (Fig. 2(a)), we need to impose four axes of control. Figure 2(b) shows the beam alignment system concept in detail. Four picomotors, two for each mirror mount (New Focus Model 8807), provide the four axes of control in each arm. Each picomotor has a step size of $\sim 30\ \text{nm}$, which translates into an angle resolution of $\sim 0.75\ \mu\text{rad}$ and a beam angle adjustability of $\sim 1.5\ \mu\text{rad}$. Despite of its high resolution, a picomotor is inherently a non-deterministic device,⁵ hence must be used with feedback if precision control is required.

A grating splits the incoming laser into two beams. Compared to a cube beamsplitter, the grating provides greater tolerance over the laser's spatial incoherence,⁶ as well as its temporal incoherence. We choose to explain the alignment process in the left arm, noting that the alignment for the right arm proceeds in a similar fashion. While aligning the left arm, the right beam is temporarily blocked. After being reflected by the two picomotor-mounted mirrors, the beam is incident upon a custom cube beamsplitter, which is mounted on the stage. The interface of the splitter is aligned parallel to the stage interferometer mirror, which is perpendicular to the substrate. After transmitting through the beamsplitter, another cube splits the beam in two, both of which fall onto position sensing detectors (PSD). A PSD not only provides a voltage readout of an incident beam's intensity, but also the beam's centroid location on the detector. The optical design is such that one of the PSD's is used to sense the incident beam's angle and the other the beam's position.⁵ Signals from the PSD's are fed into an I/O controller, which provides the feedback to the picomotors through a picomotor driver (New Focus Model 8732).

If we align the left and right beams to the same locations on both the position and angle sensing PSD's, they then overlap in position, but not necessarily on the substrate, and have equal angles of incidence. Subsequent calibrations are needed to ensure that the beams overlap in the substrate plane. This is done via the use of a third PSD, windowless and mounted on the stage, whose face is carefully positioned to the same plane as the top surface of the substrate. The positioning can be done by adjusting the PSD mount so that the reflected beam from the PSD surface aligns with that from the substrate surface.

The position and angle sensors are On-Trak Photonics UV2L2 duolateral PSD's. They are $2 \times 2 \text{ mm}^2$ in dimension. Analog inputs are handled by a National Instruments (NI) board with 16-bit A/D. When taking into consideration the position and angle decoupling topologies (discussed in more detail in the next section), we calculate the position sensor resolution to be $\sim 61 \text{ nm}$ per axis and the angle sensor resolution to be $\sim 56 \text{ nrad}$ per axis. The New Focus picomotor driver is controlled via external TTL signals from a NI digital I/O board. All control software is written in LabVIEW.

III. ITERATIVE ALIGNMENT

Figure 3 depicts the optical layout of a general-purpose beam alignment system. We have adopted the position and angle decoupling topologies discussed in one of our papers.⁶ Though other topologies may also be used, the theme remains the same: a position PSD senses only beam position fluctuations in a position decoupling plane, and an angle PSD senses only beam angle shifts at an angle decoupling plane. In our case, the SBIL beam alignment system uses the following set of physical parameters: $f_1 = 270.5$ mm, $f_2 = 540.9$ mm, $L_1 = 405.6$ mm, $L_0 = 2 L_1$ and $L_2 = f_2$. Together, these parameters determine the position and angle resolutions presented at the end of the previous section. It should be noted that the positioning tolerance on the angle decoupling lens is quite lenient.

The so-called iterative beam alignment principle is intuitive. For the same amount of angle change at the angle decoupling plane, Mirror M1 shifts the position (in the position decoupling plane) more than M2. In our setup for example, for the same $1.5 \mu\text{rad}$ beam angle change, the position shift due to M1 is $\sim 1.8 \mu\text{m}$, and that due to M2 is $\sim 1.2 \mu\text{m}$. On the other hand, for the same amount of position shift in the position decoupling plane, M2 changes the angle (at the angle decoupling plane) more than M1. Therefore, one can get a desired alignment result by iteratively using M1 to align position and M2 to align angle.

We now develop a mathematical formalism which can be used to design general iterative beam alignment systems. As we shall see, the speed at which the alignment converges to the desired angle and position is a strong function of D_1 and D_2 (Fig. 3), the distance from M1 to the position decoupling plane and the distance from M2 to the position decoupling plane, respectively.

For simplicity, we consider beam alignment using one dimensional position and angle sensors. The results we derive can be easily generalized to systems using two-dimensional sensors. Suppose initially the beam spot in the position decoupling plane is at a distance Δ from a desired position, and the beam at the angle decoupling plane makes an angle that differs by $\Delta\theta$ from a desired angle. Consider an algorithm where one iteration involves first aligning the beam's position and then angle. At the start of the first iteration, we actuate M1 to zero position, after which, the respective outputs in the position and angle decoupling planes become

$$O_p^{(1,1)} = 0, \quad (1)$$

$$O_a^{(1,1)} = \Delta\theta + \frac{\Delta d}{D_1}. \quad (2)$$

The first iteration is complete after we actuate M2 to zero angle, with outputs

$$O_p^{(1,2)} = D_2 \left(\Delta\theta + \frac{\Delta d}{D_1} \right), \quad (3)$$

$$O_a^{(1,2)} = 0. \quad (4)$$

One can easily verify that after the n -th iteration, the position and angle outputs are

$$O_p^{(n,1)} = 0, \quad (5)$$

$$O_a^{(n,1)} = \left(\frac{D_2}{D_1} \right)^{n-1} \left(\Delta\theta + \frac{\Delta d}{D_1} \right), \quad (6)$$

$$O_p^{(n,2)} = \left(\frac{D_2}{D_1} \right)^{n-1} \left(D_2 \Delta\theta + \frac{D_2}{D_1} \Delta d \right), \quad (7)$$

$$O_a^{(n,2)} = 0. \quad (8)$$

It is evident that for $D_2 < D_1$, we have convergence in both angle (Eq. 6) and position alignment (Eq. 7). The speed of convergence is directly a function of the ratio of D_2 to D_1 —the smaller the ratio, the faster the convergence.

For completeness, we give output expressions for the other iterative alignment algorithm, where an iteration is defined by first zeroing the beam's angle and then position:

$$O_p^{(n,1)} = \left(\frac{D_2}{D_1} \right)^{n-1} (D_2 \Delta\theta + \Delta d), \quad (9)$$

$$O_a^{(n,1)} = 0, \quad (10)$$

$$O_p^{(n,2)} = 0, \quad (11)$$

$$O_a^{(n,2)} = \left(\frac{D_2}{D_1} \right)^{n-1} \left(\frac{D_2}{D_1} \Delta\theta + \frac{\Delta d}{D_1} \right). \quad (12)$$

Once again, the speed of convergence is a function of the ratio of D_2 to D_1 .

Let $r \equiv D_2/D_1$. Define R to be the ratio of the desired alignment tolerance to the initial displacement (either in position or angle), e.g., if the initial displacement from a desired position is 1 mm, and the desired position alignment tolerance is 10 μm , then $R = 100$. Then the number of iterations, n , is related to r and R by

$$n \approx \log_r(R). \quad (13)$$

If one knows the desired performance specifications (n and R values), Eq. 13 can be used to calculate r, from which, the optical design for the iterative beam alignment system can proceed.

It must be pointed out that other alignment schemes do exist, for example, those based on the principle of decoupling matrix.^{5,6} The main advantage for the decoupling matrix approach is its speed. Assuming one has a controller that can drive all axes in parallel and has obtained a sufficiently accurate decoupling matrix, it is possible that one can align the beam's position and angle in a single operation. However, in our current setup, only one picomotor driver is available and the four picomotors in each arm must be addressed in a serial fashion. The speed advantage for the decoupling matrix approach becomes less obvious, because to prevent the spots from falling off the sensors, we may have to break a single alignment operation into multiple ones. Furthermore, a decoupling matrix is usually only valid for regions of the sensors that have been previously calibrated. Alignment accuracy and speed may decrease dramatically if we attempt to align spots that fall outside these regions. Iterative alignment, on the other hand, works for the full position and angle ranges as long as the beams remain on the sensors.

IV. EXPERIMENTAL RESULTS AND DISCUSSION

The beam steering system,⁶ which we use to stabilize the laser pointing, has a measured angular noise of $\sigma_{\text{ang}} = 3.8 \mu\text{rad}$. The distance between the two position decoupling planes, one for the steering system and the other for the alignment system, is about 3 m. The expected position noise is $\sigma_{\text{pos}} \approx 12 \mu\text{m}$, which is what was measured.

We must determine through a series of repeatability experiments whether or not we can align the mean beam angle and position to better than the noise present. Recall that our goals are to overlap the mean beam positions to approximately $10 \mu\text{m}$ and to equalize the mean beam angles to within $10 \mu\text{rad}$.

Figure 4 shows the results from 52 sets of alignment repeatability experiments, conducted using the left arm of the lithography interferometer. In each experiment, the spots are commanded to return to the origins on both the position and angle sensing PSD's. The alignment is complete when the program senses that the mean position has returned to

within a full σ_{pos} from the origin and the mean angle has returned to within $\sigma_{\text{ang}}/2$. The time interval dedicated to sensing the means in between consecutive picomotor commands is 0.1 seconds, at a sampling rate of 10 kHz. When the alignment is complete, a 5 second-long data set is sampled. The means from this data set are used to plot Figure 4.

All position means fall within the $\sigma_{\text{pos}} = 12 \mu\text{m}$ circle as commanded. Most of the angle means fall within the $\sigma_{\text{ang}}/2 = 1.9 \mu\text{rad}$ circle. Small spill-overs are observed, caused most likely by inaccuracies in determining the means while the alignment is still in progress. Recall that the picomotors enable a beam angle adjustability of approximately $1.5 \mu\text{rad}$. The fact that we could align the mean angle to $\sim 2 \mu\text{rad}$, which is much smaller than the required $10 \mu\text{rad}$ tolerance, means that we are aligning to the picomotor resolution.

V. CONCLUSIONS

We have described a system for carrying out automated beam alignment for scanning beam interference lithography (SBIL). A mathematical formalism has been developed to describe the iterative beam alignment principle, which can be used to guide the design of such systems. Repeatability experiments show that our system can align the mean beam angle and position to tolerances of $\ll 10 \mu\text{rad}$ and $\sim 10 \mu\text{m}$. This fulfills the alignment requirements for nanometer-level SBIL writing.

VI. ACKNOWLEDGMENTS

We gratefully acknowledge the outstanding technical assistance of James Carter, Robert Fleming and Edward Murphy. Student, staff, and facility support from the MIT Space Nanotechnology Laboratory and the MIT NanoStructures Laboratory are also appreciated. This work was supported by DARPA under Grant No. DAAG55-98-1-0130 and NASA under Grant No. NAG5-5271.

REFERENCES

- ¹ M. L. Schattenburg *et al.*, J. Vac. Sci. Technol. B **17**, 2692 (1999).
- ² C. G. Chen *et al.*, J. Vac. Sci. Technol. B **19**, 2335 (2001).
- ³ C. Joo *et al.*, submitted to J. Vac. Sci. Technol. B (2002).
- ⁴ R. K. Heilmann *et al.*, J. Vac. Sci. Technol. B **19**, 2342 (2001).
- ⁵ C. G. Chen *et al.*, Proceedings from ASPE 2001 annual meeting **25**, 216 (2001).
- ⁶ P. T. Konkola, C. G. Chen, R. K. Heilmann, and M. L. Schattenburg, J. Vac. Sci. Technol. B **18**, 3282 (2000).

FIGURES

FIG. 1. Alignment-induced phase error occurs when the substrate is unflat.

FIG. 2. SBIL beam alignment system. (a) Four degrees of freedom defining an incident beam.
(b) System concept.

FIG. 3. Design for a general beam alignment system.

FIG. 4. Beam alignment results.

Fig. 1 C. G. Chen et al.

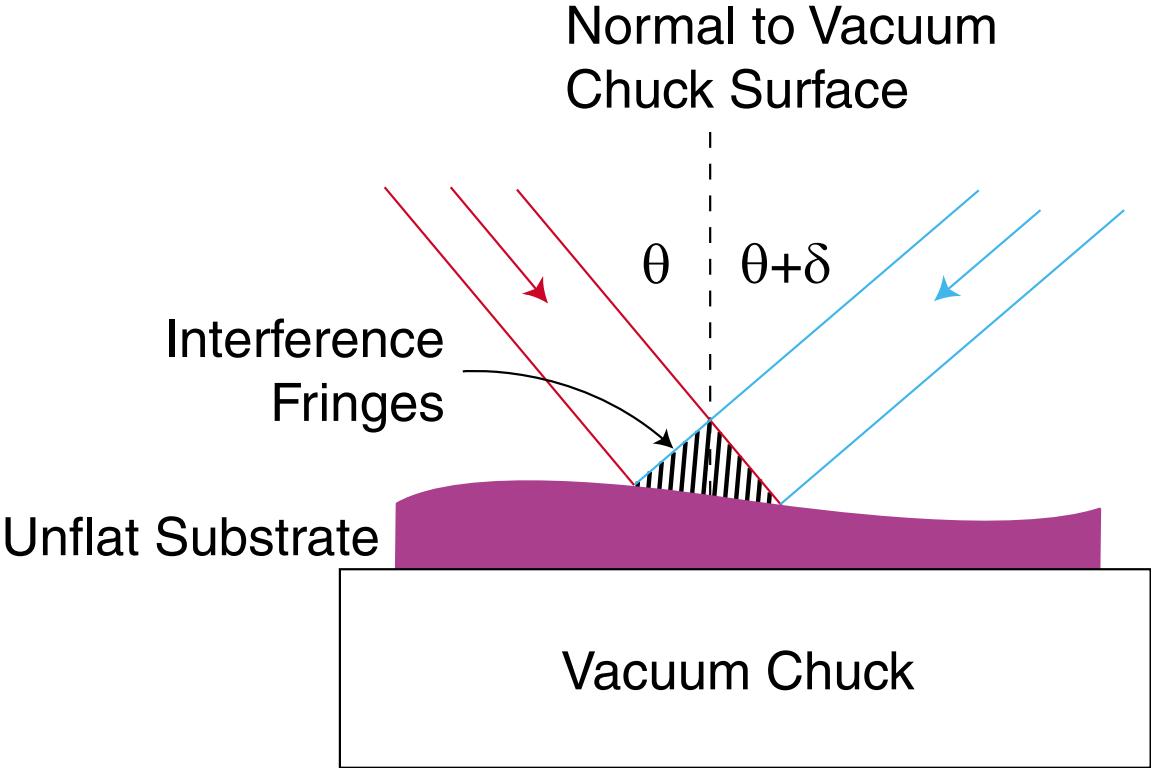
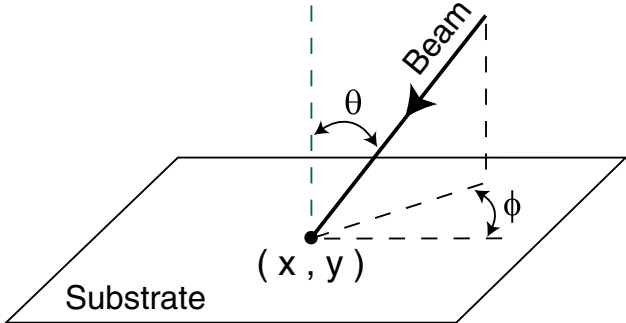
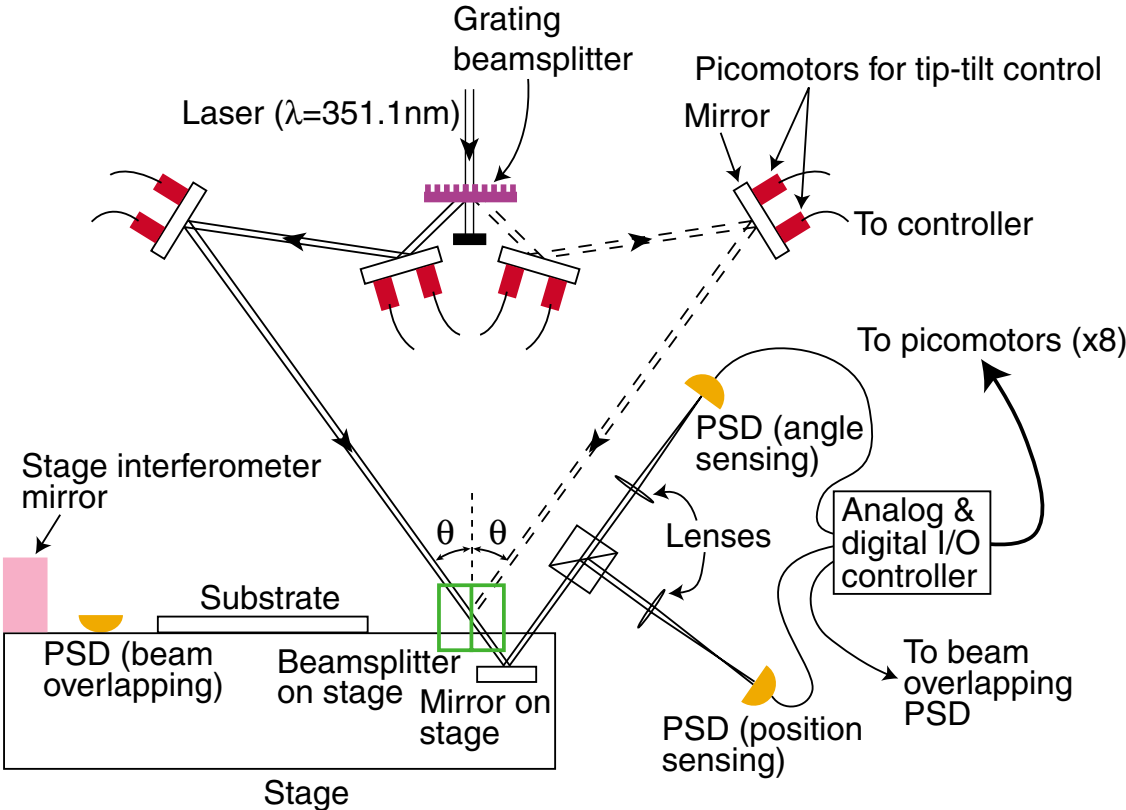


Fig. 2 C. G. Chen et al.



(a)



(b)

Fig. 3 C. G. Chen et al.

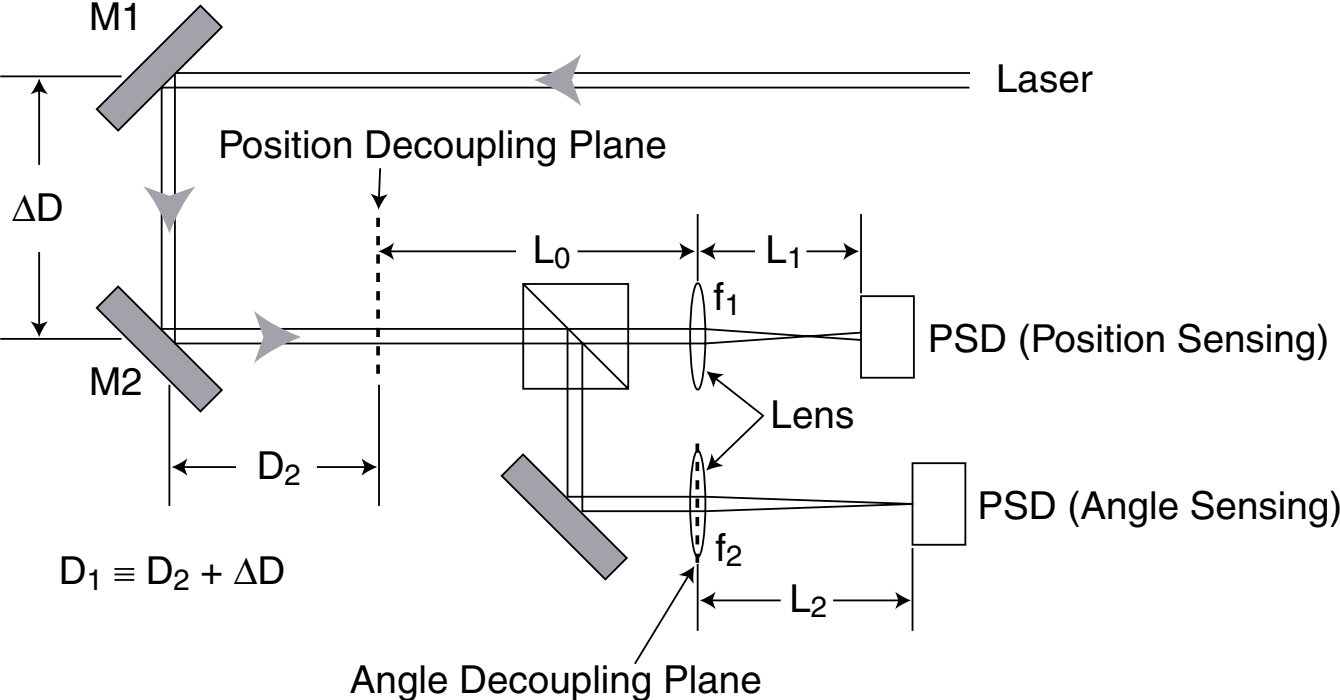


Fig. 4 C. G. Chen et al.

